

Selective photolabeling of proteins using photoactivatable GFP

George H. Patterson and Jennifer Lippincott-Schwartz*

Cell Biology and Metabolism Branch, National Institute of Child Health and Human Development, National Institutes of Health, Bethesda, MD 20892, USA

Accepted 6 October 2003

Abstract

Today's cell biologists rely on an assortment of advances in microscopy methods to study the inner workings of cells and tissues. Among these advances are fluorescent proteins which can be used to tag specifically and, in many cases, non-invasively proteins of interest within a living cell. Introduction of DNA encoding the fluorescently tagged protein of interest into a cell readily allows the visualization of the protein's localization and time-lapse imaging allows the movement of the structure or organelle to which the protein is localized to be observed. To monitor the movement of the protein within the population, researchers generally have to highlight a pool of molecules by perturbing the steady-state fluorescence. This perturbation has traditionally been performed by photobleaching the molecules within a selected region of the cell and monitoring the recovery of molecules into this region or the loss of molecules within other regions. Fluorescent proteins are now available, which allow a pool of molecules to be highlighted directly by photoactivation. Here, we discuss the technical aspects for using one of these recently developed photoactivatable fluorescent proteins, PA-GFP.

Published by Elsevier Inc.

1. Introduction

Fluorescence microscopes and fluorophores provide a straightforward approach to localize a molecule of interest within a cell. While localization offers the investigator important insight, kinetic microscopy methods, such as time-lapse imaging, look beyond a snapshot and visualize the movement of the fluorescently tagged molecule of interest in the context of a living cell. Coupled with the phenomena of photobleaching (fluorescence depletion) or photoactivation (fluorescence enhancement) to manipulate selectively the fluorescence, time-lapse imaging can also show the movement of the molecule within its steady-state population. The availability of commercial instruments capable of easily performing these techniques and the development of genetically encoded fluorescent protein markers have made these approaches widely available in the cell biology community.

Photobleaching is the photo-induced destruction of a fluorophore and has been used extensively to monitor

fluorescent molecule movement. Photoactivation, on the other hand, is traditionally associated with the photo-induced release of a caging group from an inert caged compound to produce an active molecule [1]. The addition of a caging group to a fluorophore renders the molecules non-fluorescent when excited at its normal excitation wavelength. Excitation or photoactivation with light of ~ 350 nm breaks the photolabile bond between the caging group and the fluorophore. Excitation at the normal excitation wavelength then leads to a new population of fluorescent molecules, which contrast with a background of dark molecules. The methods associated with fluorophore photobleaching [2] and uncaging by photoactivation [3] are discussed elsewhere. Here, the technical aspects of using photoactivatable green fluorescent protein (PA-GFP) to highlight selectively molecules of interest are discussed [4].

2. Photoactivatable fluorescent proteins

Photoactivatable fluorescent proteins offer an approach similar to photoactivation of caged fluorophores, yet these markers do not require the addition of

* Corresponding author.

E-mail address: lippincj@mail.nih.gov (J. Lippincott-Schwartz).

a caging group and retain the advantage of being genetically encoded. A number of proteins that are capable of photoactivation are listed in Table 1. These proteins are from various species and require different conditions for photoactivation, but they have the same general characteristic of emitting higher levels of fluorescence after photoactivation than before photoactivation. The photoactivatable proteins listed in the table include:

wtGFP, which photoconverts under ultraviolet irradiation [5,6]; several *Aequorea victoria* variants that under low oxygen conditions convert into red fluorescent species upon irradiation with 488 nm light [7,8]; the red fluorescent asFP595 [9] and its newer version, KFP1[10]; DsRed, which has green fluorescence that can be enhanced by 3-photon photobleaching of its red fluorescent component [11]; Kaede [12], which exhibits a

Table 1
Photoactivatable fluorescent proteins

Protein	Fold-activation	Wavelengths (nm) (post-activation)		Organism of origin	Reference
		λ_{ex}	λ_{em}		
wtGFP	3	481	505	<i>Aequorea victoria</i>	Irradiation with 365 nm laser light was used for local fluorescence enhancement [6]
wtGFP		~525	560–600	<i>Aequorea victoria</i>	Irradiation with 488 nm laser light under low oxygen conditions produces a red fluorescent protein [7]
GFPmut1		~525	560–600	<i>Aequorea victoria</i>	Irradiation with 488 nm laser light under low oxygen conditions produces a red fluorescent protein [7]
GFPmut2		~525	560–600	<i>Aequorea victoria</i>	Irradiation with 488 nm laser light under low oxygen conditions produces a red fluorescent protein [7,8]
GFPmut3		~525	560–600	<i>Aequorea victoria</i>	Irradiation with 488 nm laser light under low oxygen conditions produces a red fluorescent protein [7]
GFP S65T		~525	560–600	<i>Aequorea victoria</i>	Irradiation with 488 nm laser light under low oxygen conditions produces a red fluorescent protein [7]
GFP I167T		~525	560–600	<i>Aequorea victoria</i>	Irradiation with 488 nm laser light under low oxygen conditions produces a red fluorescent protein [7]
GFPuv		~525	560–600	<i>Aequorea victoria</i>	Irradiation with 488 nm laser light under low oxygen conditions produces a red fluorescent protein [7]
asFP595 (asCP)		568	595	<i>Anemonia sulcata</i>	[9]
drFP583 (DsRed)		558	583	<i>Discosoma</i> sp.	3-photon photobleaching of red species in mixed green and red tetramers leads to an increase in green fluorescence [11]
PA-GFP	101	504	517	<i>Aequorea victoria</i>	Irradiation with 413 nm laser light or Hg ²⁺ lamp (405/40X excitation filter) was used for photoactivation [4]
Kaede	2000	572	582	<i>Trachyphyllia geoffroyi</i>	Irradiation with 405 nm laser light or xenon lamp (365 nm or 400 nm) was used for optical marking [12]
KFP1	30	580	600	<i>Anemonia sulcata</i>	Irradiation with 532 nm laser light, 543 nm laser light, or a lamp (TRITC filter) was used for kindling [10]

>2000-fold increase in its red-to-green fluorescence ratio upon photoactivation; and PA-GFP [4]. While the methods described here for PA-GFP may be adapted for the use of these other photoactivatable fluorescent proteins, the various technical aspects of each protein must be considered.

3. PA-GFP background

The *A. victoria* wtGFP normally has a major absorbance peak at ~ 400 nm and a minor peak at ~ 475 nm. Irradiation of the 400 nm peak leads to a decrease in absorbance at this wavelength and an increase in absorbance in the 475 nm wavelength region. By imaging using 488 nm laser light, this phenomenon was utilized by Yokoe and Meyer [6] to locally enhance the fluorescence of wtGFP. This photo-induced conversion of wtGFP provided the basis for the development of PA-GFP [4]. The rationale was to find a mutation that decreased absorbance at 488 nm while still permitting photoconversion. Mutagenesis of the threonine at the 203 position to an isoleucine was known to reduce the minor absorbance peak while retaining a peak at ~ 400 nm [13,14]. Several other substitutions at this po-

sition were found to decrease minor peak absorbance and, surprisingly, maintained the ability to undergo photoconversion [4]. The T203H mutant (Fig. 1) exhibited the most contrast between pre- and post-photoactivation fluorescence of the mutants screened and was termed PA-GFP [4]. Before photoactivation, the native PA-GFP has a major absorbance peak at 399 nm with a slightly red-shifted fluorescence emission (~ 517 nm) compared with EGFP (data not shown). After photoactivation, a new major absorbance peak is observed at ~ 504 nm, but the ~ 517 nm fluorescence emission peak is maintained under ~ 475 nm excitation.

4. PA-GFP techniques

The use of PA-GFP requires two separate components: photoactivation and imaging. Once the protein is photoactivated, the excitation and emission peaks of PA-GFP (Fig. 1; open circles and open squares) are only slightly red-shifted compared with class 2 variants such as the S65T and enhanced GFP (EGFP) [15]. Therefore, while imaging of photoactivated PA-GFP is fairly straightforward with most currently available instruments, the requirement of uncommon excitation filters or laser lines makes the photoactivation more technically challenging.

5. Locating positive cells and structures

Prior to photoactivation, the PA-GFP displays very little fluorescence. Unless a stable cell line is produced, even finding a cell expressing the PA-GFP tagged protein of interest can be problematic. However, native PA-GFP emits with green fluorescence when excited with low levels of ~ 400 nm light (data not shown). With a quantum yield of only ~ 0.13 [4], native PA-GFP fluorescence is dim, but is usually sufficient to locate positive cells and structures. Care must be taken to minimize the exposure time when irradiating at this wavelength because this will lead to premature photoactivation and decrease the maximum attainable contrast between pre- and post-photoactivated PA-GFP. Alternatively, co-transfection with a second red or cyan fluorescent protein can be used to locate transfected cells. Members of our laboratory currently use the monomeric red fluorescent protein, mRFP1 [16].

6. Photoactivating PA-GFP

PA-GFP photoactivation requires a separate excitation source or at least a different filter set than that used for imaging. The photoactivation wavelength dependence has not been rigorously determined but it is

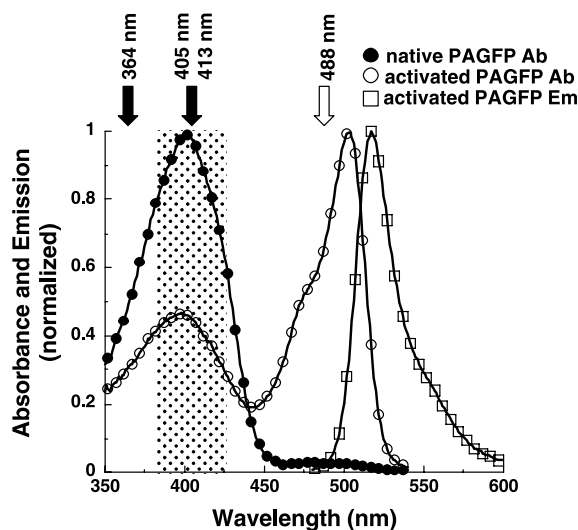


Fig. 1. PA-GFP absorbance and emission spectra. PA-GFP was His₆-tagged, expressed in bacteria, and purified from the bacterial lysate by affinity chromatography. Native PA-GFP absorbance spectrum is represented by the solid circles. PA-GFP was placed in a cuvette and photoactivated by irradiation with 25 mW 413 nm laser light for 30 min at room temperature. The photoactivated PA-GFP absorbance spectrum is shown in open circles. The native PAGFP emission spectrum is not shown because it closely resembles the photoactivated PA-GFP emission spectrum under 475 nm excitation, which is shown in the open squares. The wavelengths of light known to photoactivate PA-GFP are indicated by the black arrows (laser lines: 364, 405 or 413 nm) or by the hatched region (D405/40X band pass filter used with a Hg²⁺ lamp). The common 488 nm laser line used for imaging photoactivated PA-GFP is indicated by the white arrow.

assumed to closely resemble the native PA-GFP absorbance spectrum. The major absorbance peak of native PA-GFP is located at ~ 400 nm with the band encompassing the range from ~ 350 to 450 nm (Fig. 1; closed circles). Thus far, photoactivation has been obtained by irradiation into this band with a number of different laser lines (black arrows in Fig. 1) and at least one fluorescence excitation filter (hatched area in Fig. 1), albeit with different efficiencies.

7. Imaging the photoactivated PA-GFP

Photoactivated PA-GFP has a major excitation peak at 504 nm and very little absorbance at the 514 nm line of an argon ion laser. Therefore, users are generally limited to the 488 nm laser line or a fluorescein-like filter set and Hg^{2+} lamp for excitation. If imaging PA-GFP alone, a long pass emission filter (we use LP505) should be used to maximize the amount of fluorescence collected. If imaging in combination with a longer wavelength dye or fluorescent protein, we usually use a band pass filter (BP505-530 or BP505-550).

Unlike conventional fluorescent proteins in which the starting level of fluorescence is usually the highest level that will be observed, the level of PA-GFP fluorescence after photoactivation must be estimated to avoid detector saturation at a given imaging excitation power and detector gain. Some trial and error with various detector gain settings (contrast or voltage settings) will be required initially. A simple procedure for estimation of post-photoactivation fluorescence involves taking a pre-photoactivation image, measuring the mean fluorescence within the region to be photoactivated, background subtracting that mean and multiplying that number by the maximum attainable level of photoactivation (in the case of PA-GFP expressed in cells, ~ 60). This will give a rough estimation of the pixel values after photoactivation. In most cases, this will be an overestimation since the level of attainable contrast may be decreased by previous 400 nm light exposure when locating a positive cell or structure.

8. Typical photoactivation experiment

Once the region of interest in an expressing cell is located and the 488 nm laser power and detector gain are adjusted for the expected fluorescence increase, the experiment is similar to a fluorescence recovery after photobleaching (FRAP) experiment. A time-lapse image experiment is set up, which has the following series of events. (1) The cell is initially imaged 1–10 times with ~ 488 nm excitation. This can be done with the 488 nm line of an argon ion laser or with fluorescein-like filter sets and a Hg^{2+} lamp. (2) The irradiation wavelength is

switched to ~ 400 nm. This can be one of the laser lines indicated in Fig. 1 or with a Hg^{2+} lamp and an excitation filter with a band pass similar to the one indicated in Fig. 1. (3) The region of interest is irradiated. Selectively photoactivating the region is more easily performed by scanning with a laser line only within that region. However, a Hg^{2+} lamp with a pinhole can probably be used as well, albeit with less efficiency and temporal resolution. (4) Excitation is switched back to ~ 488 nm and the cell is imaged until the end of the experiment. Once photoactivated in this fashion, the absorbance and emission characteristics are constant and do not return to those of the pre-photoactivation state (data not shown).

9. Optimizing photoactivation

Regardless of the excitation source, some effort must be expended to obtain optimal photoactivation. Photoactivation of PA-GFP is dependent on the duration of excitation power per unit area. Although a similar approach can be taken with cells expressing PA-GFP, the dependence on power and duration is most easily demonstrated and optimized *in vitro* using His₆-tagged PA-GFP protein expressed in and purified from bacteria (Fig. 2). By embedding purified PA-GFP in

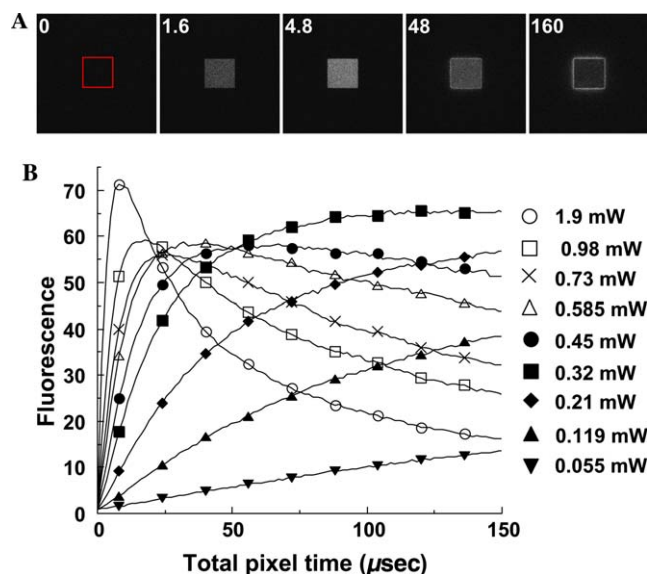


Fig. 2. Photoactivation of PA-GFP. (A) Purified PA-GFP embedded in 15% polyacrylamide was repeatedly imaged using 488 nm excitation. Between images, the region indicated in the square was irradiated with 413 nm laser light. The total pixel time of irradiation is shown in the upper left corner of the image. (B) PA-GFP embedded in polyacrylamide was repeatedly imaged and irradiated with different levels of 413 nm light. The indicated powers were measured at the back aperture of the objective. The 488 nm excited fluorescence within the photoactivated region was normalized to the initial value and displayed as a function of the accumulated pixel time.

polyacrylamide between a standard microscope slide and coverslip, an immobile, homogeneous sample of reproducible protein concentration is obtained. Excitation of the embedded PA-GFP with 488 nm laser light produces little fluorescence (Fig. 2A; time 0 μ s) until irradiation of the region indicated by the square in Fig. 2A with 413 nm light. In this experiment, the entire field of immobilized protein was repeatedly imaged with 488 nm light while the region indicated by the square was irradiated with 413 nm light between images. The pixel dwell time during photoactivation was held constant at 1.6 μ s and the images in Fig. 2A are displayed as the total accumulated photoactivation time per pixel. In the example in Fig. 2, \sim 1.9 mW of 413 nm laser power was used at the back aperture of a Carl Zeiss 63X 1.4 NA Plan-Apochromat objective. After 1.6 μ s photoactivation pixel time, a modest level of fluorescence increase is obtained. After three iterations (4.8 μ s total pixel time), full activation can be obtained. At longer irradiation times in Fig. 2, the photoactivated PA-GFP fluorescence is depleted within the region and is surrounded by a bright fluorescent rim. This loss in fluorescence is not due to photobleaching during 488 nm imaging since little fluorescence loss is observed after a single photoactivation event followed by 488 nm imaging (data not shown). Therefore, the decrease in photoactivated PA-GFP fluorescence is due to photobleaching by the repeated exposures to 413 nm laser light.

Photobleaching is encountered during any PA-GFP photoactivation experiment. Therefore, to maximize the contrast between pre- and post-photoactivation, power and duration of the photoactivation must be optimized such that the highest level of photoactivation is obtained

with the least amount of photobleaching. The dependence of photoactivation and photobleaching on the 413 nm irradiation power and duration is shown in Fig. 2B. The graphical representation of the images in Fig. 2A shows that the level of fluorescence increases exponentially to an apex and then decreases over longer pixel time periods. The levels of activation obtained with the accumulated pixel time due to multiple iterations closely mimic a single iteration of the same pixel time (data not shown). Since the apex of one of the curves in Fig. 2B represents the highest level of obtainable photoactivation, we define this point as the total pixel time required for optimal photoactivation. As shown in Fig. 2B, decreasing the 413 nm laser power at the back aperture of the objective shifts the apex to longer accumulated pixel time. Therefore, to perform the photoactivation event as rapidly as possible, the maximum available power should be used. Of course, the temporal requirements will be dependent on the dynamics of the photoactivation target.

The excitation power duration per unit area is altered with each change in objective or zoom factor. This dependence is shown in Fig. 3 with data from experiments similar to that in Fig. 2 performed using three different objectives at three different zoom factors. Each data point in Fig. 3 represents the pixel time at the apex of a photoactivation curve for the laser power and zoom factor indicated. The solid lines represent linear fits from $\log(\text{power})$ versus $\log(\text{pixel time})$ plots (not shown). As anticipated, these graphs show that the increased zoom factor, which effectively increases the pixel time per unit area, shifts the pixel time and power required for optimal photoactivation to lower values.

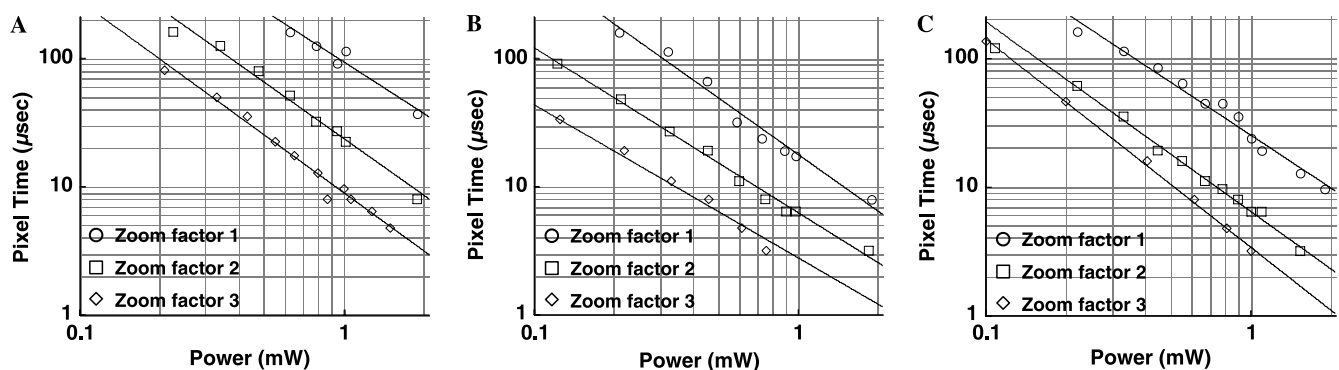


Fig. 3. Photoactivation dependence on the duration of excitation power per unit area. Purified PA-GFP was embedded in polyacrylamide and repeatedly imaged and photoactivated at various power levels as in Fig. 2. These experiments were performed using three different objectives at three different zoom factors. (A) Each data point represents the apex of a photoactivation curve as shown in Fig. 2B performed using a Carl Zeiss 25X Plan-Neofluar 0.8 NA objective at zoom factor 1 ($0.72 \mu\text{m} \times 0.72 \mu\text{m}$ pixel size) represented by the open circles, zoom factor 2 ($0.36 \mu\text{m} \times 0.36 \mu\text{m}$ pixel size) represented by the open squares, and zoom factor 3 ($0.24 \mu\text{m} \times 0.24 \mu\text{m}$ pixel size) represented by the open triangles. (B) Each data point represents the apex of a photoactivation curve as shown in Fig. 2B performed using a Carl Zeiss 63X Plan-Apochromat 1.4 NA objective at zoom factor 1 ($0.29 \mu\text{m} \times 0.29 \mu\text{m}$ pixel size) represented by the open circles, zoom factor 2 ($0.14 \mu\text{m} \times 0.14 \mu\text{m}$ pixel size) represented by the open squares, and zoom factor 3 ($0.1 \mu\text{m} \times 0.1 \mu\text{m}$ pixel size) represented by the open triangles. (C) Each data point represents the apex of a photoactivation curve as shown in Fig. 2B performed using a Carl Zeiss 100X Plan-Apochromat 1.4 NA objective at zoom factor 1 ($0.18 \mu\text{m} \times 0.18 \mu\text{m}$ pixel size) represented by the open circles, zoom factor 2 ($0.09 \mu\text{m} \times 0.09 \mu\text{m}$ pixel size) represented by the open squares, and zoom factor 3 ($0.06 \mu\text{m} \times 0.06 \mu\text{m}$ pixel size) represented by the open triangles. The solid lines through each data set represent linear fits of \log - \log plots of the power and pixel times.

The photoactivation data provided in Fig. 3 may be used as a quick reference for new experimenters using PA-GFP. These values can only be strictly applied to experiments using the same objectives and same photoactivation wavelength, but the fits shown in the solid lines should provide a rough guide for obtaining optimal photoactivation with most systems. For example, assuming ~ 1 mW at the back aperture of the 63X Plan-Apochromat 1.4 NA objective in Fig. 3B, ~ 6 μ s of total pixel time for pixels of ~ 0.02 μ m² size (zoom 2) is required for optimal photoactivation. Use of power levels or excitation duration above the solid line will lead to increased photobleaching as shown in Fig. 2. Use of power levels or excitation duration below the line will lead to inefficient photoactivation. Thus, using the proper power level and duration is essential to maximize the pre- versus post-photoactivation contrast. Differences in objective parameters such as the efficiency of light transmission, numerical aperture, and the size of the back aperture in addition to the wavelength of photoactivation light will shift the power versus duration dependence.

The use of Fig. 3 as a guide requires prior knowledge of the laser power available at the back aperture of the objective. For this, a power meter is generally required. Some currently available confocal microscopes have internal meters to monitor day-to-day laser powers. However, handheld power meters are available from many laser manufacturers and are relatively inexpensive compared with a confocal microscope purchase. For the experiments in Figs. 2 and 3, an objective was removed and the 413 nm laser power at the nosepiece was measured at several levels controlled by an acousto optical tunable filter (AOTF).

Alternative to measuring excitation power, experimenters can simply optimize photoactivation in a manner similar to that described in Fig. 2 for each set of parameters. Since the same parameters (objective, zoom factor, and photoactivation wavelength) may be used on a daily basis for most experiments, a single optimization routine may suffice. This assumes that day-to-day fluctuations in laser power and alignment are minor. Of course, if the excitation source is replaced, realigned, or loses power over time, the optimization step should be repeated.

10. Conclusions and future directions

PA-GFP complements and extends the more common photobleaching techniques applied to the study of protein behavior within living cells [2]. However, other photoactivatable fluorescent proteins listed in Table 1

have been developed that show great promise for use in cell biology. Since they exhibit red fluorescence and high contrast between their photoactivated and native states, Kaede and KFP1 bear particular attention. As imaging tools, PA-GFP, Kaede, and KFP1 have some disadvantages, such as the near ultraviolet excitation required for photoactivation of PA-GFP and Kaede and the self-association properties of Kaede and KFP1 [17]. We anticipate that future work with these proteins will produce improved molecules that lack many of the pitfalls currently encountered and will make them even more easily utilized for monitoring protein, organelle, and cell behavior.

Acknowledgments

We thank Peter Kim and Eileen Whiteman for critical reading of the manuscript. G.P. was an Intramural Research Training Award fellow during this work.

References

- [1] J.C. Politz, *Trends Cell Biol.* 9 (1999) 284–287.
- [2] J. Lippincott-Schwartz, N. Altan-Bonnet, G.H. Patterson, *Nat. Cell Biol.* 5 (2003) S7–S14.
- [3] T.J. Mitchison, K.E. Sawin, J.A. Theriot, K. Gee, A. Mallavarapu, in: S.P. Colowick, G. Marriot (Eds.), *Methods in Enzymology*, Academic Press, San Diego, 1998, pp. 63–78.
- [4] G.H. Patterson, J. Lippincott-Schwartz, *Science* 297 (2002) 1873–1877.
- [5] M. Chatteraj, B.A. King, G.U. Bublitz, S.G. Boxer, *Proc. Natl. Acad. Sci. USA* 93 (1996) 8362–8367.
- [6] H. Yokoe, T. Meyer, *Nat. Biotechnol.* 14 (1996) 1252–1256.
- [7] M.B. Elowitz, M.G. Surette, P.-E. Wolf, J. Stock, S. Leibler, *Curr. Biol.* 7 (1997) 809–812.
- [8] K.E. Sawin, P. Nurse, *Curr. Biol.* 7 (1997) R606–R607.
- [9] K.A. Lukyanov, A.F. Fradkov, N.G. Gurskaya, M.V. Matz, Y.A. Labas, A.P. Savitsky, M.L. Markelov, A.G. Zarausky, X. Zhao, Y. Fang, W. Tan, S.A. Lukyanov, *J. Biol. Chem.* 275 (2000) 25879–25882.
- [10] D.M. Chudakov, V.V. Belousov, A.G. Zarausky, V.V. Novoselov, D.B. Staroverov, D.B. Zorov, S. Lukyanov, K.A. Lukyanov, *Nat. Biotechnol.* 21 (2003) 191–194.
- [11] J.S. Marchant, G.E. Stutzmann, M.A. Leissring, F.M. LaFerla, I. Parker, *Nat. Biotechnol.* 19 (2001) 645–649.
- [12] R. Ando, H. Hama, M. Yamamoto-Hino, H. Mizuno, A. Miyawaki, *Proc. Natl. Acad. Sci. USA* 99 (2002) 12651–12656.
- [13] R. Heim, D.C. Prasher, R.Y. Tsien, *Proc. Natl. Acad. Sci. USA* 91 (1994) 12501–12504.
- [14] T. Ehrig, D.J. O’Kane, F.G. Prendergast, *FEBS Lett.* 367 (1995) 163–166.
- [15] R.Y. Tsien, *Annu. Rev. Biochem.* 67 (1998) 509–544.
- [16] R.E. Campbell, O. Tour, A.E. Palmer, P.A. Steinbach, G.S. Baird, D.A. Zacharias, R.Y. Tsien, *Proc. Natl. Acad. Sci. USA* 99 (2002) 7877–7882.
- [17] J. Lippincott-Schwartz, G.H. Patterson, *Science* 300 (2003) 87–91.